

Wave Amplification inside an Open Circular Caisson for Wave Energy Conversion in Waters with Medium Energy Density

Chin-Hung Yao and Jiahn-Horng Chen

Abstract—Wave energy is one of important marine renewable energy resources. Many studies have been devoted to harnessing the energy for human use. Though they are almost everywhere in the sea, waves can be much more significant in some sea areas than others. To make the wave energy harvesting more viable in waters with less significant waves, we propose to employ an open caisson to amplify the wave locally and to combine it with a wave energy converter to tap the amplified wave energy. In this study, we focus on the effect of incident wave height on the amplification factor which is defined as the ratio of the wave height inside the caisson to that of the incident wave. The study was conducted primarily by CFD computations and partially verified by experiments. It is interesting to find that the amplified wave height in the caisson is not linearly related to the incident wave height. Furthermore, the amplification factor is also a function of the incident wave period. The wave period at which the peak value of the amplification factor appears is insensitive to the wave height. The amplification factor is always greater than unity for a wide range of incident wave period.

Keywords—Caisson, harbour resonance, nonlinear effect, wave energy amplification.

I. INTRODUCTION

WAVE energy is one of the most abundant renewable energy resources around the world. It attracts global interest to develop wave energy conversion technologies. There have been many types of wave energy converters (WECs) developed in the past several decades [1-2]. Each type has its own advantages and disadvantages. For example, the OWC (oscillating water column) type of WEC can have better survivability under extreme wave conditions, but the fixed type of OWSCs (oscillating wave surge converters) have higher capture width ratios. As far as the technical capabilities are

concerned, none of them exceeds the others. More efforts on technological advance are required to tap the wave energy economically for commercial operations.

In addition to technological issues, further concerns need be considered if the wave energy is to be harnessed in low-latitude waters. In these areas, the wave energy density is relatively small. Therefore, the energy which can be effectively harnessed could also be small. The cost per unit power captured could be seriously high. Nevertheless, in these areas, there usually exist tropical cyclones such as hurricanes and typhoons. The extreme sea condition often makes WECs vulnerable under the extreme loading conditions [3-4].

To deal with such a dilemma, we have studied a type of device, consisting of a cylindrical caisson with a constant side opening from the top to the bottom and a WEC inside it, for wave energy conversion. For wave to propagate into the caisson, part of the caisson's side wall is cut and removed. By the principle of harbour resonance [5], the wave inside the caisson can be significantly magnified if its geometrical dimensions are properly specified for some particular wave conditions and water depth [6-7]. Since the wave energy density is proportional to the square of the wave height, the wave power inside the caisson is much more amplified. This enhances the wave energy harvest with a suitable WEC. Furthermore, the caisson can also play the role to protect the WEC inside it in extreme weather as caissons are usually made with reinforced concrete, much stronger than the WEC itself.

The fundamental phenomena on harbour resonance have been exhaustively investigated and various formulae derived for simple geometries [8]. Many studies were restricted to the linear realm. Some focused on nonlinear effects. Rogers [9] considered a long narrow rectangular harbour of constant depth and developed a nonlinear potential-flow theory of wave oscillations in it. He found that the resonant amplification of the first harmonic decreased with increasing incident wave amplitudes. He also concluded that the linearized theory overestimated the resonant response of a harbour subject to monochromatic incident waves. Such a phenomenon was also observed in the experiments of a circular harbour with linear incident waves [10]. The amplification varies with the wave height of the incident wave. Later, Lepelletier and Raichlen [11] also proposed a

©2023 European Wave and Tidal Energy Conference. This paper has been subjected to single-blind peer review.

C.-H. Yao is with Shih Yen-Ping Center for Underwater Technology, National Taiwan Ocean University, 2 Pei-Ning Road, Keelung, 202, Taiwan (e-mail: b0105@mail.ntou.edu.tw).

J.-H. Chen is with Shih Yen-Ping Center for Underwater Technology, National Taiwan Ocean University, 2 Pei-Ning Road, Keelung, 202, Taiwan (e-mail: jhchen202@gmail.com).

Digital Object Identifier: <https://doi.org/10.36688/ewtec-2023-164>.

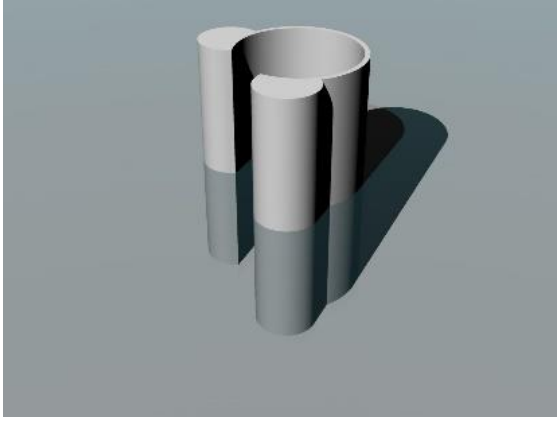
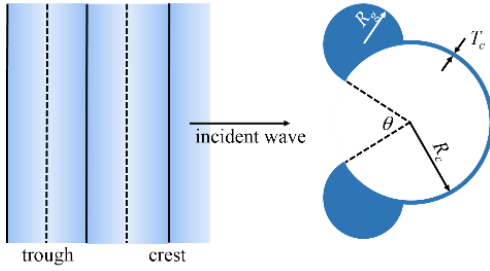
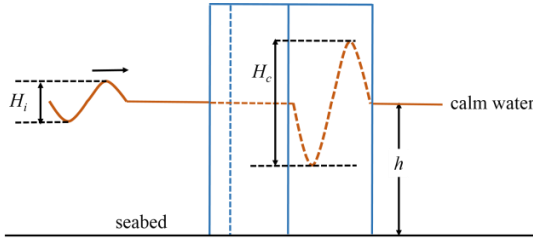


Fig. 1. The caisson for the present study.



(a) Top view.



(b) Frontal view.

Fig. 2. Schematic of the present study.

nonlinear, dispersive, dissipative model for waves in rectangular tanks. Comparing the results by a linear model, they showed that the linear theory was inadequate to describe the physics near the resonant mode of oscillations. Other nonlinear phenomena inside the harbour were also studied by, e.g., Dong *et al.* [12], Losada *et al.* [13], Gao *et al.* [14], Gao *et al.* [15], and Marcos, *et al.* [16].

Since our purpose is to enhance the wave energy harvest by an open cylindrical caisson, it is vital to understand how the wave height affects the wave amplification inside the caisson. In the present study, we conducted a series of viscous flow computations to investigate the relation between the incident wave height and the wave amplification for various incident wave periods. In addition, we also attempted to reveal how the amplification is related to the vortex dynamics due to the existence of several vortices when water moves into and out of the caisson. Some interesting phenomena will be discussed in the following.

II. PHYSICAL PROBLEM AND NUMERICAL APPROACH

A. Physical problem

In this paper, we study the wave amplification inside a caisson with an opening shown in Fig. 1. The caisson is mounted vertically on the horizontal seabed in the open sea. At the edge of the opening, it has two guides on the two sides of the opening. They are identical in geometry and part of a solid cylinder. The purpose of the two guides is to enhance the wave amplification inside the caisson [6-7]. To define the physical parameters, Fig. 2 shows the top and frontal views of the caisson. The linear wave of height H_i and period T approaches the caisson. The caisson has an opening of angle θ . The water depth is h . The radii of the caisson and the guides are R_c and R_g , respectively. The thickness of the caisson wall is T_c . The wave inside the caisson is amplified and its wave height at the centre of the caisson is H_c . We define the amplification factor

$$R = \frac{H_c}{H_i}. \quad (1)$$

The hydrodynamic phenomena involved in this problem can be described by the three-dimensional Navier-Stokes equations

$$\nabla \cdot \mathbf{u} = 0 \quad (2)$$

$$\rho \left(\frac{\partial}{\partial t} + \mathbf{u} \cdot \nabla \right) \mathbf{u} = \rho \mathbf{g} - \nabla p + \mu \nabla^2 \mathbf{u} \quad (3)$$

where \mathbf{u} and p represent the velocity and pressure fields, respectively, \mathbf{g} the gravity, t the time, ρ the water density, and μ the dynamic viscosity of water. The velocity \mathbf{u} is a vector which can be expressed as $\mathbf{u} = u\mathbf{i} + v\mathbf{j} + w\mathbf{k}$ with u , v , and w the velocity components in the streamwise, lateral, and vertical directions, respectively. We include the viscous effect in the present study in order to investigate how the vortical flow affects the wave amplification inside the caisson.

Several boundary conditions need be specified for well-posedness of the problem. Far upstream, the incoming wave can be expressed as

$$u = \frac{H_i}{2} \omega \frac{\cosh k(h+z)}{\sinh(kh)} \cos(kx - \omega t + \varphi) \quad (4)$$

$$w = \frac{H_i}{2} \omega \frac{\sinh k(h+z)}{\sinh(kh)} \sin(kx - \omega t + \varphi) \quad (5)$$

where ω is the wave angular frequency, k wave number, and φ the phase angle. The relation between T and ω is $T = 2\pi/\omega$. On the caisson surfaces and seabed, the no-slip condition is specified. On the free surfaces, the

dynamic and kinematic boundary conditions should be specified. However, in the computational procedure discussed below, the two conditions will not be employed for solution; rather, the VOF (volume of fluid) approach will be used.

B. Numerical approach

To analyze the present problem, we employed CFD tools. The particular software used is the free open source code OpenFOAM. The olaFlow model based on OpenFOAM with the finite volume method approach was chosen in this study. The olaFlow model consists of a set of solvers and boundary conditions to generate and absorb water waves effectively on the boundaries and to simulate their interaction with structures inside the flow domain [17]. The SIMPLE algorithm was used for the iterations of the velocity and pressure fields and the PISO algorithm for the time marching. In addition, in the solver, the volume of fluid method was used for the treatment of the free surface.

The typical conditions at the NTOU (National Taiwan Ocean University) Ocean Energy Test Site will be employed for computations and further discussion in the following. The water depth $h = 20$ m. The typical wave period ranges between 8 and 10 s; therefore, T varies in this study from 6 s to 12 s. The typical wave height ranges between 1.5 and 3.5 m. An extended range from $H_i = 0.5$ m to 3.0 m will be our focus on studying the effect of wave height on the amplification factor. Furthermore, the best size of the caisson to amplify the incident wave at $T = 9$ s and $H_i = 2.5$ m has been studied by Chen *et al.* [18]. Their result of $R_c = 6$ m and $R_g = 3$ m will be employed for the present study. The angle θ was specified to be 60° . The physical parameters of freshwater at 20°C were used in computations.

For computations, the infinite physical domain must be truncated to reduce to a finite region. In the present study, the dimensions of the whole computational domain is 300 m in length (the streamwise direction), 240 m in width (the lateral direction), and 32.71 m in height. The caisson centre is on the symmetry plane and 180 m from the upstream boundary. The water depth is 20 m and, therefore, the height of the computational domain for the air region is 12.71 m. The structured grid combining O- and H-types was generated. The total grid number is about 2.19M. Fig. 3 shows part of the grid layout around the caisson. The time step for the unsteady computations is $\Delta t = 0.01$ s.

In addition, the absorbing boundary condition was specified on the downstream and the two side boundaries to ensure no reflection of waves due to the domain truncation in all computations. For this, we employed the active wave absorption method proposed by Schäffer and Klopman [19]. The method has been implemented in the olaFlow model.

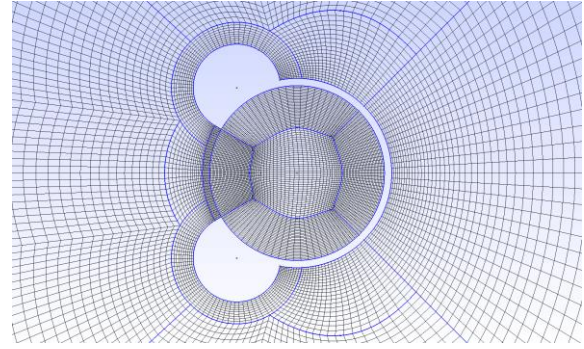


Fig. 3. Structural grid layout around the caisson.

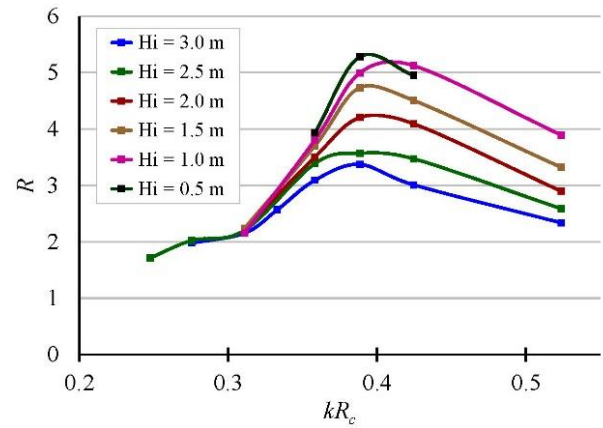


Fig. 4. Amplification factor at different wave heights and wave periods.

III. RESULTS AND DISCUSSION

In the following, we present our computational results. First of all, we will discuss the effect of the incident wave height on the wave amplification inside the caisson with a global picture. Then we examine the hydrodynamic features of the interaction between the incident wave and the caissons.

C. Amplification factor

Shown in Fig. 4 are the amplification factors R , at different incident wave periods T , and wave heights H_i . We can have several observations from these results.

First of all, for each particular wave height H_i , the value of R varies with that of kR_c . The variations are mild for $kR_c > 0.39$. This is especially true when the wave height is large. It indicates that the amplification factor is usually not very sensitive to the variation of incoming wave period. Therefore, the range of the incident wave period for effective wave energy harvest is wide. In addition, all amplification factors are greater than unity in the present study, though some are large and some not so large. The caisson can always magnify the wave energy density.

The R - kR_c curves have a peak for all wave heights in the range of present investigation. It is interesting to find that the critical value of kR_c corresponding to the peak of R for different H_i is almost the same. Its value is about 0.39. This signifies that the peak of amplification is not a

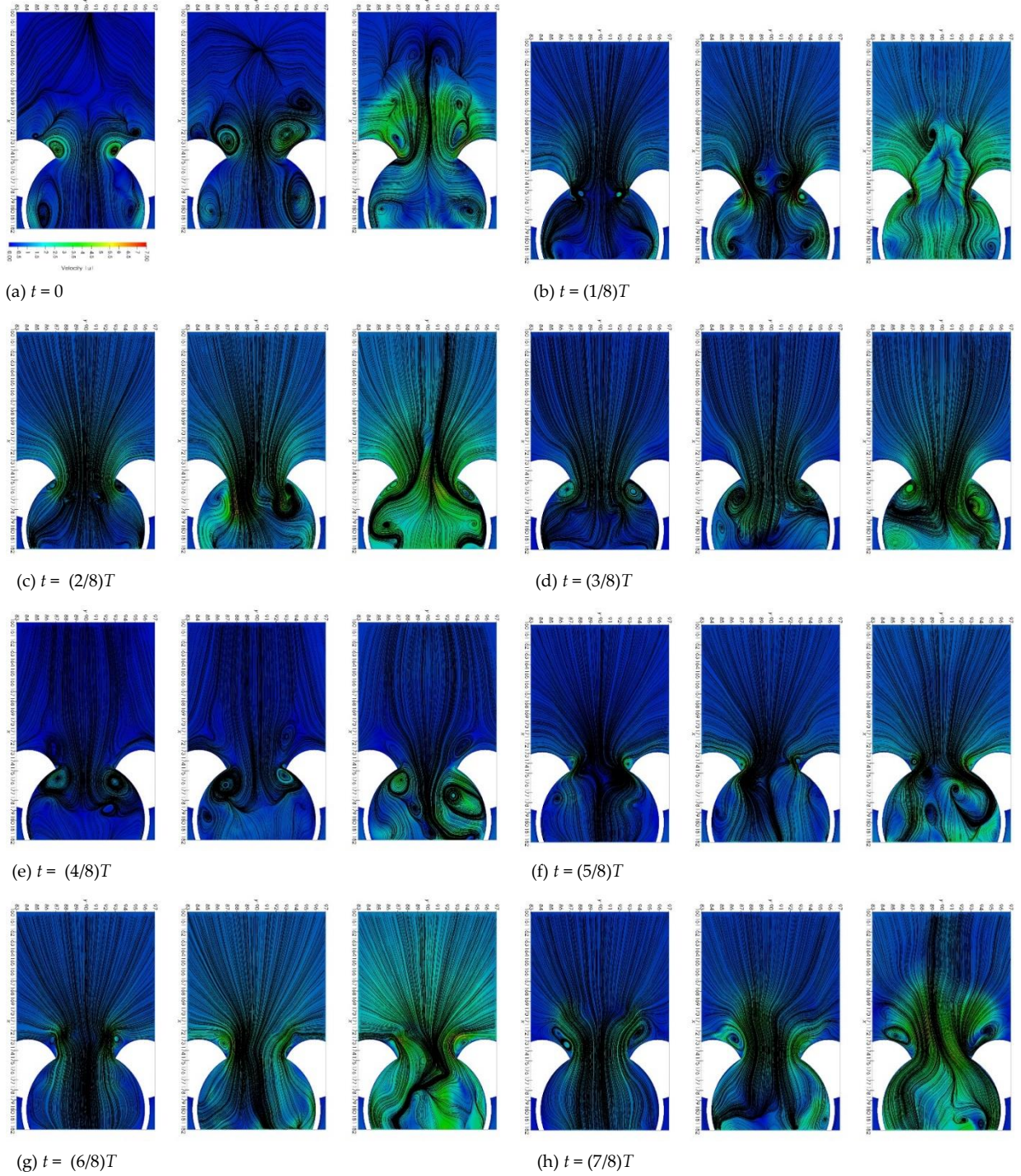


Fig. 5. The instantaneous streamlines and velocity magnitude when $H_i = 2.5$ m (in each plot, left: $z = 5$ m; middle: $z = 10$ m; right: $z = 15$ m).

function of the incident wave height H_i . Such a phenomenon was also observed in Lin *et al.* [17]. However, the critical value in the present study is different from theirs, though their difference is not significant. This could be due to the fact that the caisson radius and/or water depth are different.

Furthermore, the amplification factor R , decreases as the incident wave height H_i increases. This is consistent to what Rogers [9] and Hsu *et al.* [10] observed though the harbour which Rogers studied is different from the caisson of the present in shape. Such a trend is also beneficial to the wave power harvest because it could reduce the inherent fluctuations of wave energy harvest.

For example, if we observe the wave power density at $H_i = 0.5$ m and 3.0 m and $kR_c = 0.39$, the ratio is approximately 1:36 for waves outside the caisson and about 1:9 inside the caisson.

As a final remark, we also observe that at small value of kR_c , the curves appear to coincide with each other and the amplification factor becomes small. A small value of kR_c implies that the incident wave period becomes large. This is to say that long waves cannot be effectively amplified inside the caisson.

D. Vortex system near the caisson opening

The time variation of the vortex systems near the

caisson opening has not been discussed in the literature. Since our computations were conducted with the Navier-Stokes equations, some vortical flow can be observed. In the following, we will focus on the vortex system development at two different incident wave heights. Of particular interests are the two extreme cases in our series of computations; that is, $H_i = 0.5$ m and 2.5 m, representing the small and large waves, respectively. The vortices on three horizontal planes at $z = 5$, 10, and 15 m from the seabed will be discussed.

Fig. 5 shows the computational results for $H_i = 2.5$ m. We divided a wave period into eight equal time intervals. We then specified the time when the wave trough passed the centre of the caisson to be $t = 0$. The plots in Fig. 5 are shown in sequence at $t = 0$, $(1/8)T$, $(2/8)T$, $(3/8)T$, ..., and $(8/8)T$. In each plot, the curves are the instantaneous streamlines and the colour represents the magnitude of the instantaneous velocity.

Overall speaking, it is obvious that the flow near the free surface is much more significant. In the deeper region, the flow is slower and, hence, the vortices are small; in the region close to the water surface, the flow speed is bigger and the vortices are larger. The contribution to the wave amplification in the deeper region is then relatively minor. Most contribution comes from the region near the free surface.

Figs. 5(a)-(d) show the inflow to the caisson owing to the wave crest approaching to it. The vortices outside the caisson shown in Fig. 5(a) are destroyed and disappear very quickly. Meanwhile, the existence of the sharp edges makes the flow separate in the caisson. The vortices grow with time. The size of the vortex pair reaches its peak when the centre of the caisson aligns with the wave crest, shown in Fig. 5(e).

Around this moment, the passage for the in-flow becomes narrow because the vortices form big recirculation regions which block the inflow. Figs. 5(e)-(h) depict the stage of outflow from the caisson. At the edges of the guides, the vortices form and grow with time. The sizes also reach their peaks when the caisson center aligns with the wave trough, shown in Fig. 5(a). Around this moment, the outflow passage also becomes narrow, which is comparable to that during the inflow stage shown in Fig. 5(e). Meanwhile, the vortices on the inside of the opening are destroyed and vanish.

Fig. 5 also shows the effect of guides on the wave amplification inside the caisson. During the inflow stage (Figs. 5(a)-(d)), the flow outside the rectangular region with the opening being the cross section is guided into the caisson. That is, more water can flow into the caisson. This makes the free surface inside the caisson move further upwards. Similarly, during the outflow stage (Figs. 5(e)-(h)), the flow emits out from the caisson in the opposite direction with a larger cross section area. Therefore, the free surface within the caisson moves further downwards. In total, the wave height inside the caisson becomes even bigger. Consequently, to mount the

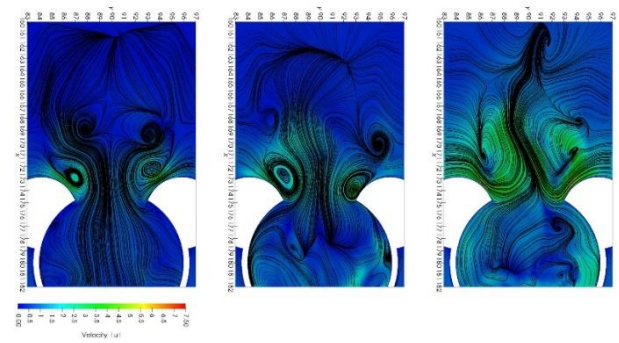


Fig. 6. The instantaneous streamlines and velocity magnitude at $t = (8/8)T$ (left: $z = 5$ m; middle: $z = 10$ m; right: $z = 15$ m).

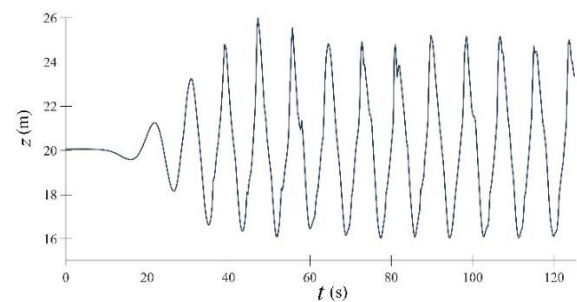


Fig. 7. The vertical position of the free surface at the caisson centre.

guides on the caisson is beneficial for wave energy harvest.

In Fig. 5, it is also obvious that the flow pattern is asymmetric at the three different depths. This phenomenon has been examined in the literature and can be explained by the instability theory of the counter-rotating vortex pair, including Crow instability for long waves [20] and elliptic instability for short waves [21]. Following Fig. 5(h) at $t = (7/8)T$, Fig. 6 shows the flow pattern at $t = (8/8)T$. Obviously, the streamlines in Fig. 6 and Fig. 5(a) are not identical to each other, though the global patterns are similar. In our computation, the results shown in Fig. 6 also reveal that at the outflow stage, the vortices may be shed from the guide surface. Fig. 7 shows the vertical position of the free surface at the caisson centre. We find that the variation in time is not periodic even though the incident wave is periodic. The peak and valley positions fluctuate in each cycle, reflecting the flow instability. However, the wave height variation is not significant.

Fig. 8 shows the computational results for $H_i = 0.5$ m at some moments. Similar to the flow phenomena for $H_i = 2.5$ m, vortices form on the inner side of the caisson for the inflow and on the guide surface for the outflow. The important difference is that for $H_i = 0.5$ m, the vortices are much smaller in size. They simply attach to the guide surface and the inner sides of the caisson. They are so small that the passages are wider than those for $H_i = 2.5$ m and do not block the inflow or outflow. The wide passages obviously reduce the flow hindrance for fluid flow into or out of the caisson. This explains the previous

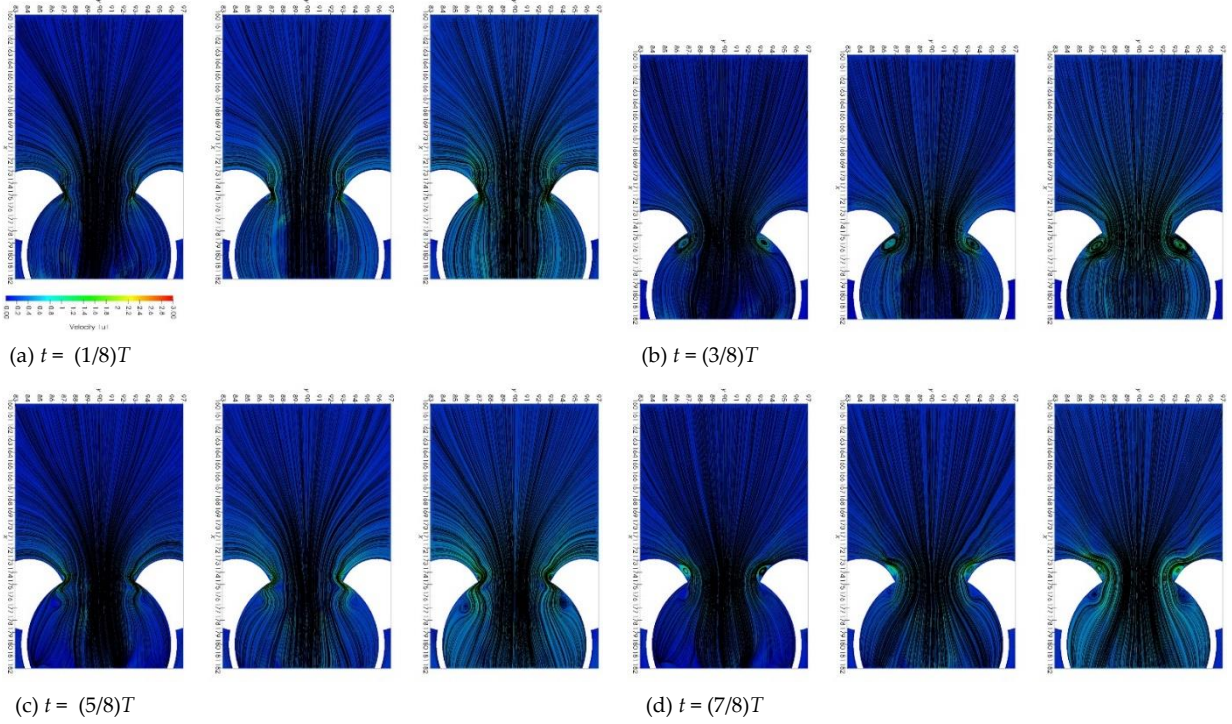


Fig. 8. The instantaneous streamlines and velocity magnitude when $H_i = 0.5$ m (in each plot, left: $z = 5$ m; middle: $z = 10$ m; right: $z = 15$ m).

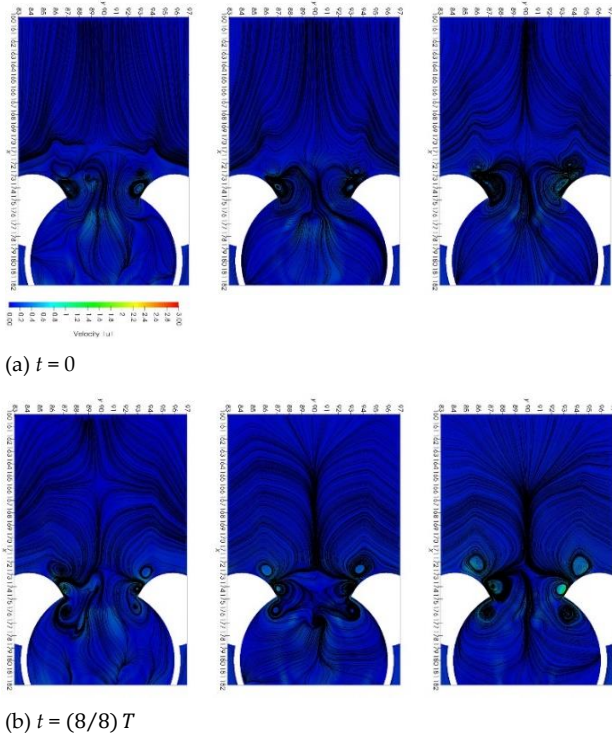


Fig. 9. The flow patterns around the caisson at times being one period apart (in each plot, left: $z = 5$ m; middle: $z = 10$ m; right: $z = 15$ m).

result that the amplification factor for the incident wave with a small wave height is larger than that with a large wave height.

Fig. 9 shows the instantaneous streamlines and velocity magnitude at $t = 0$ and $(8/8)T$. Again, they are not identical to each other due to the flow instability even though the two incoming waves are identical and exactly

one period apart in time. However, the flow topologies at the two instants are the same on the side of guide surface.

IV. CONCLUSIONS

In this paper, we have studied the wave amplification inside a caisson with a pair of guides. Different wave heights were specified and the amplification factors were found by solving the flow field with OpenFOAM, a free CFD package. The results show that the amplification factor decreases as the incident wave height increases. However, the largest amplification occurs at $kR_c = 0.39$, independent of the wave height.

We also examined the vortical flow and found that the vortices formed and grew alternately on both sides of the caisson, depending on the flow direction. If the wave height is small, the vortices are small and do not influence the flow passing the caisson opening. However, if the wave height is large, the vortices grow to an extent that the flow passage can be partially blocked.

REFERENCES

- [1] C.G. Soares, J. Bhattacharjee, M. Tello, and L. Pietra, "Review and classification of wave energy converters," in *Maritime Engineering and Technology*, 1st edition, London, UK: CRC Press, 2012, ch. 72, pp. 599-608.
- [2] I. Lopez, J. Andreu, S. Ceballos, I. Martinez de Alegria, I, and I. Kortabarria, "Review of wave energy technologies and the necessary power-equipment," *Renew. Sustain. Energy Rev.*, vol. 27, pp. 413-434, 2013.
- [3] R. Tiron, F. Mallon, F. Dias, and E.G. Reynaud, "The challenging life of wave energy devices at sea: A few points to consider," *Renew. Sustain. Energy Rev.*, vol. 43, pp. 1263-1272, 2015.
- [4] T. Aderinto and H. Li, "Ocean wave energy converters: Status and challenges," *Energies*, vol. 11, 1250, 2018.
- [5] F.M. Martinez and V.S. Naverac, "An experimental study of

- harbour resonance phenomena," in *21st International Conference on Coastal Engineering*, Costa del Sol-Malaga, Spain, 1989, pp. 270-280.
- [6] Y.-X. Lin, D.-W. Chen, and J.-H. Chen, "Interaction of wave with an open caisson," in *4th International Conference in Ocean Engineering*, Chennai, India, 2018, pp. 599-613.
- [7] Y.-X. Lin, D.-W. Chen, and J.-H. Chen, "Simulation of a resonance-amplified floater oscillation in an open-type circular caisson," in *13th European Wave and Tidal Energy Conference*, Napoli, Italy, 2019.
- [8] A.B. Rabinovich, "Seiches and harbour oscillations," in *Handbook of Coastal and Ocean Engineering*, Singapore: World Scientific Publisher, 2018, ch. 11, pp. 243-286. [Online]. Available: https://www.worldscientific.com/doi/abs/10.1142/9789812819307_0009.
- [9] S.R. Rogers, "Finite Amplitude Harbor Oscillations: Theory and Experiment," Ph.D. Dissertation, MIT, Cambridge, MA, USA, 1977.
- [10] F.-H. Hsu, J.-H. Chen, and J.-F. Tsai, "An experimental study of wave amplification inside an open caisson for harnessing wave energy," in *Oceans*, Marseille, France, 2019.
- [11] T.G. Lepelletier and F. Raichlen, "Nonlinear oscillations in rectangular tanks," *J. Eng. Mech.*, vol. 114, pp. 1-23, 1988.
- [12] G.H. Dong, G. Wang, X.Z. Ma, and Y.X. Ma, "Numerical study of transient nonlinear harbor resonance," *Sci. China Technol. Sci.*, vol. 53, pp. 558-565, 2010.
- [13] I.J. Losada, J.M. Gonzalez-Ondina, G. Diaz-Hernandez, and E.M. Gonzalez, "Numerical modeling of nonlinear resonance of semi-enclosed water bodies: Description and experimental Validation," *Coastal Eng.*, vol. 55, pp. 21-34, 2008.
- [14] J. Gao, C. Ji, O. Gaidai, and Y. Liu, "Numerical study of infragravity waves amplification during harbor resonance," *Ocean Eng.*, vol. 116, pp. 90-100, 2016.
- [15] J. Gao, C. Ji, Y. Liu, X. Ma, and O. Gaidai, "Influence of offshore topography on the amplification of infragravity oscillations within a harbor," *Appl. Ocean Res.*, vol. 65, pp. 129-141, 2017.
- [16] M. Marcos, P.L.-F. Liu, and S. Monserrat, "Nonlinear resonant coupling between two adjacent bays," *Oceans*, Vol. 109, C05008, 2004.
- [17] A. Iturrioz, R. Guanche, J.L. Lara, C. Vidal, and I.J. Losada, "Validation of OpenFOAM® for oscillating water column three-dimensional modelling," *Ocean Eng.*, vol. 107, pp. 222-236, 2015.
- [18] D.-W. Chen, Y.-X. Lin, and J.-H. Chen, "A feasibility assessment of wave energy captures on an open caisson on the northeast coastal waters of Taiwan," in *8th Advanced Maritime Engineering Conference*, Busan, Korea, 2018.
- [19] H.A. Schäffer and G. Klopman, "Review of multidirectional active wave absorption methods," *J. Waterway, Port, Coastal, Ocean Eng.*, vol. 126, pp. 88-97, 2000.
- [20] T. Leweke and C.H.K. Williamson, "Experiments on long-wavelength instability and reconnection of a vortex pair," *Phys. Fluids*, vol. 23, 024101, 2011.
- [21] T. Leweke, T. and C.H.K. Williamson, "Cooperative elliptic instability of a vortex pair," *J. Fluid Mech.*, vol. 360, pp. 85-119, 1998.